ISSN 0030-400X, Optics and Spectroscopy, 2015, Vol. 118, No. 1, pp. 11–18. © Pleiades Publishing, Ltd., 2015.
Original Russian Text © N.N. Lavrent'eva, B.A. Voronin, A.A. Fedorova, 2015, published in Optika i Spektroskopiya, 2015, Vol. 118, No. 1, pp. 13–20.

SPECTROSCOPY OF ATOMS AND MOLECULES

$H_2{}^{16}O$ Line List for the Study of Atmospheres of Venus and Mars

N. N. Lavrent'eva[a, b], B. A. Voronin[a, c], and A. A. Fedorova[d, e]

[a] *Zuev Institute of Atmospheric Optics, Siberian Branch, Russian Academy of Sciences, Tomsk, 634021 Russia*
[b] *National Research Tomsk Polytechnic University, Tomsk, 634050 Russia*
[c] *Tomsk State University of Control Systems and Radioelectronics, Tomsk, 634050 Russia*
[d] *Space Research Institute, Russian Academy of Sciences, Moscow, Russia*
[e] *Moscow Physico-Technical Institute, Dolgoprudnyi', 141700 Russia*
e-mail: lnn@iao.ru, vba@iao.ru, fedorova@iki.rssi.ru

Received May 8, 2014

Abstract—IR spectroscopy is an important method of remote measurement of $H_2{}^{16}O$ content in planetary atmospheres with initial spectroscopic information from the HITRAN, GEISA, etc., databases adapted for studies in the Earth's atmosphere. Unlike the Earth, the atmospheres of Mars and Venus mainly consist of carbon dioxide with a CO_2 content of about 95%. In this paper, the line list of $H_2{}^{16}O$ is obtained on the basis of the BT2 line list (R.J. Barber, J. Tennyson, G.J. Harris, et al., *MNRAS* **368**, 1087 (2006)). The BT2 line list containing information on the centers, intensities, and quantum identification of lines is supplemented with the line contour parameters: the self-broadening and carbon dioxide broadening coefficients and the temperature dependence coefficient at 296 K in the range of 0.001–30 000 cm^{-1}. Transitions with intensity values 10^{-30}, 10^{-32}, and 10^{-35} cm/molecule, the total number of which is 323 310, 753 529, and 2 011 072, respectively, were chosen from the BT2 line list.

DOI: 10.1134/S0030400X15010178

INTRODUCTION

One important problem in the study of the atmospheres of planets of the Earth's class is measurement of the content and distribution of water vapor. Unlike the Earth's atmosphere, the atmospheres of Mars and Venus consist of CO_2 (95.3 and 96.5%, respectively). The water cycle is one of the main climate cycles of Mars. Water is intensely transferred between the hemispheres, and its content changes from less than 1 precipitated μm to 100 precipitated μm in the summer period in the northern hemisphere. In Venus' atmosphere, the relative content of water vapor varies from 30 ppm near the surface down to 1–3 ppm in the mesosphere. Water vapor is an important chemical compound taking part in the formation of the dense cloud layer of Venus consisting of sulfuric acid. Traditionally, in studies of planetary atmospheres, constant coefficients have been used to calculate the line broadening in a carbon dioxide atmosphere. They were determined relative to the air-broadening coefficient by introducing a constant factor, which has been varied from 1.3 to 1.7 in different studies [1–5]. The values of coefficients were based on the data of [6, 7]. A variable broadening was used in some studies depending on a particular transition [8–10] on the basis of [6, 11] by R.H. Tipping and R. Freedman (private communication, see [12]). At the same time, an inaccuracy of the broadening coefficient can introduce a systematic error in the determination of water content. For example, in reconstructing the integral water-vapor content in the Martian atmosphere from data on the 20–40 μm band [2], the error was estimated to be ±25% if the broadening coefficient is varied in the interval of 1.2–1.8 with an average value of 1.5. For this error, a lower estimate of ~5% was obtained in [4] for measurements in the H_2O 1.38 μm band in the near-IR range.

At present, the instrumental base for the study of planetary atmospheres by the methods of high-resolution spectroscopy is rapidly progressing. Starting in 2006, the SOIR instrument on board the Venus Express mission has measured the water vapor using the 2.6 μm band with a resolution of 20000 (which is unparalleled in orbital measurements near another planet) [13, 14]. High-resolution terrestrial measurements of water-vapor absorption in the atmospheres of Mars and Venus have been performed [15, 16]. Experiments for the ExoMars-2016 mission are in preparation [17, 18], which will be devoted, in particular, to measurement of vertical and spatial content of water vapor and the isotope ratio H_2O/HDO in the Martian atmosphere. In conducting these studies, accurate spectroscopic information on water-vapor broadening in carbon dioxide atmospheres is required.

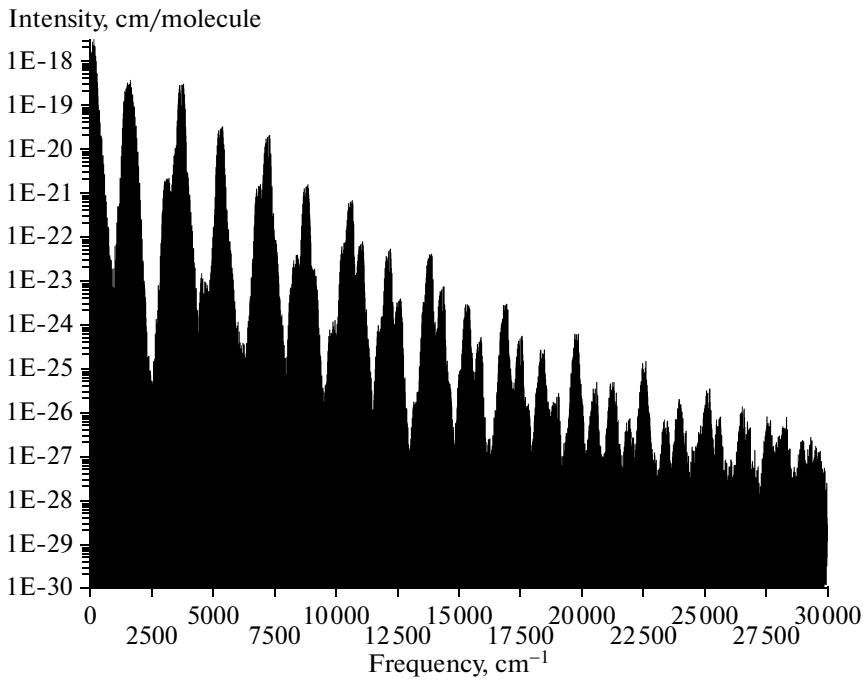

Fig. 1. General view of the BT2 line list.

CALCULATION OF THE SPECTRUM OF H_2O–CO_2

Of the existing spectroscopic databases containing H_2O, the BT2 line list [19] was recommended for the use in modeling the H_2O absorption in the lower Venusian atmosphere as the most complete and consistent with the observations of night "transparency windows" of Venus' atmosphere [20].

The BT2 was obtained by using the discrete variable representation method DVR3D [21]; it is available on the Internet (http://www.exomol.com), and contains data on more than 500 000 000 transitions in the range of up to 30000 cm^{-1}.

However, its efficient use requires sufficiently powerful computing facilities. The number of energy levels presented in the BT2 is 221 096 (for J from 0 to 50). The following information is presented for each energy level: its energy value; the number in a series; the number in a submatrix; the symmetry; quantum number J of angular momentum; and vibration–rotation labeling ν_1, ν_2, ν_3, J, K_a, and K_c. If the value of a quantum number is unknown, it is marked by "–2".

In the calculation and/or estimation of line contour parameters, knowledge of the vibration–rotation labeling is of fundamental importance. If the parameters of a contour are determined only with the use of their rotational dependence, it is necessary to know J, K_a, and K_c of the lower and upper levels.

In the BT2 line list, a complete set of quantum numbers in the normal modes, ν_1, ν_2, ν_3, K_a, and K_c, is absent for more than 70% of energy levels. In our case, with the intensity cutoff at 10^{-30}, 10^{-32}, and 10^{-35} cm/molecule, the complete set of quantum numbers is absent for 35, 50, and 62% of transitions, respectively.

The general form of the BT2 line list with the intensity cutoff at 10^{-30} cm/molecule is shown in Fig. 1.

In our calculations, we employed the a semiempirical method based on the impact theory of broadening and modified by introducing additional parameters obtained by using empirical data. The model parameters are determined by fitting the broadening and shift coefficients to the experimental values. In the calculations of line-contour parameters, we used a new approach developed in cooperation with colleagues from the University College London, in which the intramolecular effects are taken into account on the basis of accurate wave functions and energy levels obtained from variational calculations. This approach takes into account the contributions of all scattering channels induced by molecular collisions and, in addition, allows one to calculate the line-contour parameters of water up to the dissociation limit of the molecule.

In our calculations, it is necessary to know the matrix elements of the collision-induced transition dipole moment, which are calculated with the use of a dipole moment surface. The Partridge–Schwenke surface derived from ab initio calculations is the best surface. The broadening and shift coefficients of spectral lines of the water molecule induced by the pressure of different atmospheric gases were calculated by a

semiempirical method, which, like the Anderson method, contained a cutoff procedure. This method works in the approximations of the impact theory. The general assumptions in this case are that collisions are binary, the duration of collisions is shorter than the time between collisions, the translational motion of particles is described in the approximation of classical trajectories, and the line interference is not taken into account.

Earlier, we used the semiempirical method in conjunction with the method of effective Hamiltonians to calculate the line-contour parameters and the coefficients of their temperature dependence for colliding molecules H_2O–N_2, H_2O–O_2, and H_2O–H_2O.

Here, the semiempirical method is supplemented with the use of accurate variational wave functions obtained from global variational calculations. Their use not only allows us to improve the calculations of contour parameters, but also extends the region of applicability of the method up to the dissociation limit of a molecule.

A weakness of the technique adopted in our work is the use of a cutoff procedure similar to that used in the Anderson method. This approximation is valid for molecules characterized by strong interactions when the radius of the closest approach of molecules is smaller than cut off parameter, i.e., when $r_c < b_0$, where r_c is the closest approach radius and b_0 is the cutoff radius. The carbon dioxide molecule has no dipole moment, but it possesses a rather large quadrupole moment, so that $r_c > b_0$ for most collisions of the colliding system H_2O–CO_2. The influence of short-range forces is insignificant in this case and is accounted for by a correction factor.

To calculate the contributions of different scattering channels corresponding to collisional transitions, we used transition probabilities $D^2(ii'|l)$ and $D^2(ff'|l)$ reconstructed from Einstein coefficients A in the BT2 line list. We had to choose Einstein coefficients A from the 500 million values presented in the total BT2 list. In calculating the broadening and shift parameters of lines, we took into account the collision-induced symmetry-allowed scattering channels. In this approach, their number is much larger than in the method using the standard Watson's Hamiltonian. Our calculations showed that the contributions of scattering channels with $\omega_{ii'} > 700$ cm^{-1} and $K_a - K_a' > 3$ are negligible.

The general expression for the half-width is represented as follows:

$$\gamma_{if} = \mathrm{Re}\sum_{\mathrm{int}} \int d\upsilon \upsilon \int dbb\left(\frac{\upsilon}{\upsilon_c'}\right)^2 f\left(b,\upsilon, D^2\left(ii'|l_1l_2\right)\right. \\ \left. D^2\left(ffi|l_1l_2\right)\right). \quad (1)$$

Here, integral $\int d\upsilon$ is the averaging over collisions; f is a function containing quantities $D(b,\upsilon,i,i'|l_1l_2)$ connected with scattering channel $i \to i'$, which depend only on the molecular constants of an absorbing molecule; b is the initial velocity of the collision; and υ is the impact parameter. The integrand of (1) is expanded in a series, which yields

$$\gamma_{if} = A + \sum D^2\left(ii'|l_1l_2\right) P_{l_1l_2}\left(\omega_{ii'}\right) \\ + \sum D^2\left(ff'|l_1l_2\right) P_{l_1l_2}\left(\omega_{iff'}\right) + \ldots, \quad (2)$$

$$A = \frac{n}{c}\sum_2 \rho(2) \int_0^\infty \upsilon d\upsilon b_0^2(\upsilon,2),$$

$b_0(\upsilon, 2)$ is the cutoff parameter.

The efficiency functions of the channels can be represented in the form

$$P_{l_1l_2}(\omega) = P_{l_1l_2}^{ATC}(\omega)\left[1 + a_1\omega + a_2\omega^2 + \ldots\right], \quad (3)$$

and the expression in square brackets on the right-hand side of equality (3) can be written in terms of J-dependent expressions, parameters of which are fitted to the experimental half-width values.

The correction factor in (3) was obtained in the following form:

$$C_l = \frac{c_1}{c_2\sqrt{j_f} + 1}, \quad (4)$$

where c_1 and c_2 are adjustable parameters. The form of the correction factor is determined from analysis of the rotational dependence of the half-widths of CO_2 lines.

In the case of H_2O–CO_2 collisions, the main contribution to the broadening and the shift is made by the interaction between the dipole moment of the water molecule and the quadrupole moment of the carbon dioxide molecule. In addition, we take into account the higher-order electrostatic interactions—the quadruple–quadrupole, induction, and dispersion interactions. The quadrupole–quadrupole contribution (which is smaller than 5%) was taken into account with the use of Watson's Hamiltonian method.

The calculated results and the experimental data [22, 23] are compared in Table 1, where the broadening coefficients are presented as functions of line frequency. The experimental data were obtained for the rotational band [22] and the ν_2 band [23].

A crude estimate of the broadening coefficients of H_2O–CO_2 lines is often obtained by multiplying the air-broadening data by a certain coefficient. In [24], in interpreting the spectra of the Martian atmosphere in the IR range of 20–40 μm, the coefficient was taken to be 1.5. A value of 1.3 was used in [25] for the 1.38 μm band, and the factor was set to be 1.7 in [23]. Other values of the coefficient have been used for the atmo-

Table 1. Experimental, calculated, and estimated data: broadening coefficients γ of $H_2{}^{16}O–CO_2$

Frequency, cm^{-1}	Rotational quantum numbers		γ (CO_2), cm^{-1} atm^{-1}				Δγ (CO_2), cm^{-1} atm^{-1}			
	J', *Ka*', *Kc*'	*J*", *Ka*", *Kc*"	[22]	[7]	*JJ*'-dependence	γ CO_2 semiempirical method	[22], [7]	[22], *JJ*'-dependence	[22], γ (air) × 1.7	[22], semiempirical method
18.577	1 1 0	1 0 1	0.2156	0.2094	0.2122	0.2136	0.0062	0.0034	0.0354	0.002
32.954	2 0 2	1 1 1	0.2247	0.201	0.1796	0.2066	0.0237	0.0451	0.0510	0.0105
25.085	2 1 1	2 0 2	0.1937	0.1961	0.1975	0.2142	−0.0024	−0.0038	0.0227	−0.0129
55.702	2 1 2	1 0 1	0.1812	0.1807	0.1482	0.1948	0.0005	0.0329	0.0034	−0.0137
40.988	2 2 0	2 1 1	0.1731	0.1598	0.1642	0.1948	0.0133	0.0089	0.0068	−0.0095
55.405	2 2 1	2 1 2	0.1781	0.1729	0.1482	0.1411	0.0052	0.0299	0.0088	−0.0197
57.265	3 0 3	2 1 2	0.1917	0.1682	0.1224	0.1609	0.0235	0.0693	0.0345	0.0065
38.464	3 1 2	2 2 1	0.1831	0.1784	0.1796	0.1826	0.0047	0.0035	0.0116	−0.0117
36.604	3 1 2	3 0 3	0.1705	0.1624	0.1041	0.1949	0.0081	0.0664	0.0010	0.0077
72.188	3 1 3	2 0 2	0.1449	0.1384	0.1224	0.1778	0.0065	0.0225	−0.0193	−0.0154
38.791	3 2 1	3 1 2	0.1566	0.1535	0.1796	0.1978	0.0031	−0.0229	−0.0117	0.0155
73.262	3 3 0	3 2 1	0.1974	0.1955	0.1975	0.1507	0.0019	−6E−05	0.0216	0.0026
78.918	3 3 1	3 2 2	0.164	0.1732	0.1642	0.0991	−0.0092	−0.0001	−0.0046	0.0031
40.282	4 2 2	4 1 3	0.1489	0.1117	0.0894	0.1852	0.0372	0.0595	−0.0073	0.0072
53.444	4 1 3	4 0 4	0.1168	0.1295	0.0894	0.1603	−0.0127	0.0274	−0.0391	−0.0169
68.063	4 3 1	4 2 2	0.1471	0.1384	0.1041	0.158	0.0087	0.0429	−0.0091	−0.0059
69.196	4 1 3	3 2 2	0.159	0.1524	0.1224	0.1576	0.0066	0.0366	0.0036	0.001
75.524	4 2 3	4 1 4	0.1402	0.1362	0.1348	0.1014	0.004	0.0054	−0.0218	−0.0174
79.774	4 0 4	3 1 3	0.1764	0.1732	0.1642	0.1167	0.0032	0.0123	0.0050	−0.0014
82.155	4 3 2	4 2 3	0.1594	0.1524	0.1482	0.0929	0.007	0.0112	0.0061	0.0087
74.11	5 1 4	5 0 5	0.1381	0.1238	0.1041	0.1283	0.0143	0.0339	−0.0171	0.0098
47.053	5 2 3	5 1 4	0.119	0.1141	0.1224	0.1628	0.0049	−0.0034	−0.0369	0.0176
89.583	5 2 4	5 1 5	0.1073	0.1069	0.0781	0.0888	0.0004	0.0292	−0.0357	−0.0036
62.301	5 3 2	5 2 3	0.1193	0.1206	0.1482	0.153	−0.0013	−0.0289	−0.0320	0.0202
59.868	6 2 4	6 1 5	0.1274	0.1267	0.1348	0.1337	0.0007	−0.0074	−0.0341	0.0107
58.775	6 3 3	6 2 4	0.1045	0.1079	0.1224	0.1417	−0.0034	−0.0179	−0.0420	0.0116
78.196	7 2 5	7 1 6	0.1041	0.1265	0.0781	0.1109	−0.0224	0.0259	−0.0450	−0.0058
88.881	7 4 3	7 3 4	0.1033	0.1044	0.1041	0.1099	−0.0011	−0.0008	−0.0402	0.0145
CKO							0.0035	0.0178	0.0183	0.0037

sphere of Venus: 1.56 in [26] and a value of 1.7. For comparison, we presented the root-mean-square deviations of half-widths of air-broadened H_2O lines taken from the database HITRAN-2012 [27] and multiplied by 1.7 from the half-widths measured in [22]. Data with this factor appeared to be closest to the experimental and calculated values presented in Table 1. Large values of root-mean-square deviations are indicative of significant errors in using such crude estimates in calculations of the spectra.

The root-mean-square deviations are shown in the last four columns. It is seen that our calculation by the semiempirical method reproduces the data with almost the experimental accuracy, whereas the use of the *JJ*'-dependence for the calculations leads to a worse result.

It was already mentioned above that the complete set of quantum numbers is absent in the BT2 for many transitions. In this case, we cannot use the semiempirical method and must invoke other methods for deter-

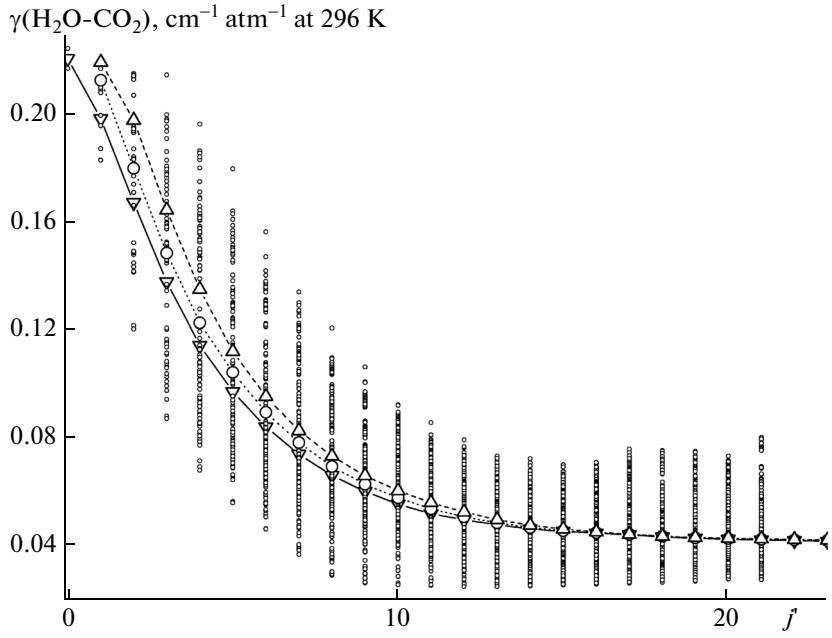

Fig. 2. Broadening coefficients of water-vapor lines induced by carbon dioxide pressure. ○—the semiempirical approach; -∇-—the *JJ*' dependence, *R* branch; -○-—the *JJ*' dependence, *Q* branch; and –Δ–—the *JJ*' dependence, *P* branch.

mining the line-contour parameters. Earlier [28–30], the *JJ*'-method was proposed for determining the air-broadening of lines for which the complete set of quantum numbers is absent but the values of angular momentum for upper and lower states (*J* and *J*') are known, as well as the symmetry of the upper and lower levels.

Figure 2 presents line half-widths $\gamma(H_2{}^{16}O–CO_2)$ calculated by the semiempirical method for different rotational quantum numbers *J*. In addition, *JJ*' estimates of the broadening coefficients for the *P*, *Q*, and *R* branches are presented for high values of angular momentum and for transitions for which the complete set of quantum numbers is absent. One can see that the difference between the values obtained by the two methods is large and can exceed 100%. However, if the complete set of quantum numbers in the normal modes is absent, the *JJ*' estimation of line half-widths provides the best results.

Figure 3 shows the broadening coefficients versus the line number (the line number increases with the line frequency). The figure displays the experimental data measured in the rotational band [22], the data measured in the ν_2 band [23], and our calculated results obtained using both the semiempirical method and the *JJ*' dependences. The average discrepancy between our results and measured half-widths $\gamma(H_2{}^{16}O–C^{16}O_2)$ from [22] is 7.9% with a maximum discrepancy of 22.3%; the analogous discrepancies from the measured data [23] are 7.3 and 13.3%, respectively.

The exponents of the temperature dependence of line half-widths of water vapor induced by carbon dioxide pressure were calculated for each line in the presented range. For rotational transitions with the complete set of quantum numbers (circles in Fig. 4), the temperature exponents were calculated by the semiempirical method. For transitions without the complete set of rotational quantum numbers or/and

Table 2

File	Size	Intensity cutoff, cm/molecule	Number of transitions	Number of transitions without identification
IntE-30-BT2-296-Venus	34 M	10^{-30}	323310	115123
IntE-32-BT2-296-Venus	80 M	10^{-32}	753529	381392
IntE-35-BT2-296-Venus	211 M	10^{-35}	2011072	1255506
readVenus.me	1801 byte			

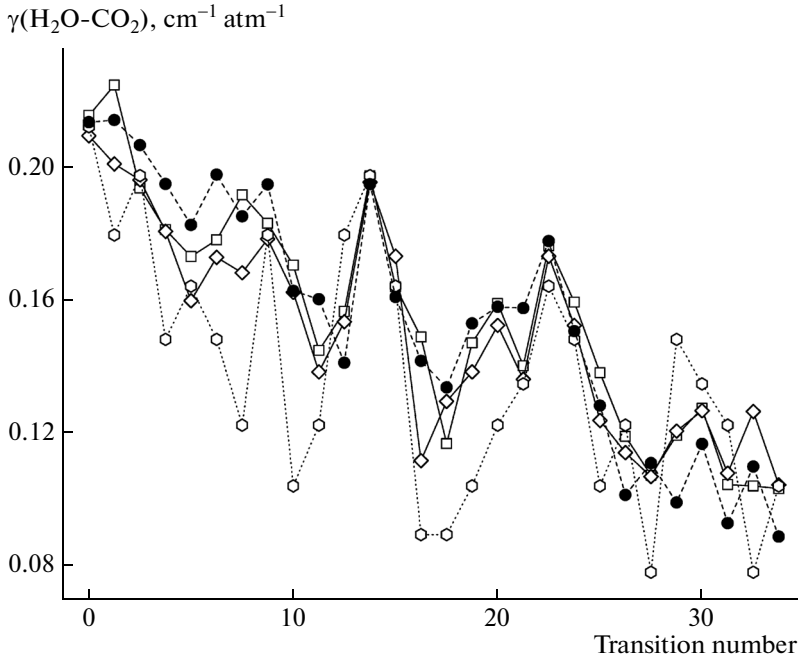

Fig. 3. Calculated and measured broadening coefficients of water-vapor lines induced by carbon dioxide pressure. □—experiment [22], ◇—experiment [23], ○—the JJ' dependence, and ●—the semiempirical calculation.

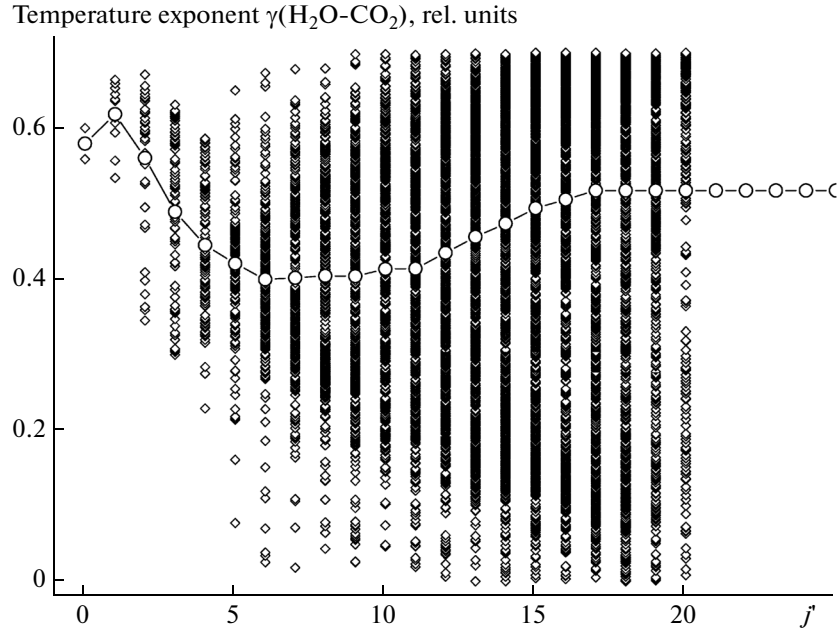

Fig. 4. Coefficients of temperature dependence (○) calculated by the semiempirical method and (–◇–) estimated using the J dependence.

transitions with large values $J > 20$ (joined black circles), we used the J dependence (Fig. 4).

In the calculations, we used the ordinary power law, and the broadening coefficients were calculated at temperatures $T = 230$, 260, 296, 320, and 350 K with reference temperature $T_0 = 296$ K. The obtained values of temperature dependence coefficients are presented in Fig. 4. The values of temperature exponents

calculated by the semiempirical method vary from 0.65 to 0.28.

The calculated data are available at the website ftp://ftp.iao.ru/pub/VTT/H2O-BT2-HW/BT2-296-Venus/. The database was constructed as follows. From the BT2, we chose transitions with intensity values of $\leq 10^{-30}$, 10^{-32}, and 10^{-35} cm/molecule, the total numbers of which are 323 310, 753 529, and 2 011 072, respectively (Table 2).

Each file contains the frequency (cm^{-1}), intensity (cm/molecule), vibration–rotation quantum identification and symmetry of the upper and lower energy levels, the energy value of a lower level (cm^{-1}), the broadening coefficient $\gamma(H_2{}^{16}O-CO_2)$ in cm^{-1}/atm, the self-broadening coefficient $\gamma(H_2{}^{16}O-H_2{}^{16}O)$ from [28], and the temperature dependence coefficient of $\gamma(H_2{}^{16}O-CO_2)$.

The BT2 line list containing information on the line centers, intensities, and quantum identification was supplemented in the range of 0.001–30000 cm^{-1} with line-contour parameters such as the self-broadening and carbon dioxide broadening coefficients and the temperature dependence coefficient at 296 K. The line broadening coefficients of water vapor induced by carbon dioxide pressure were calculated for rotational quantum number J from 0 to 50. For transitions with the complete set of quantum numbers in the normal modes, the calculations were performed by the semiempirical method. In other cases, the data were found using the JJ' dependence. The coefficients of the temperature dependence were determined for each line. All the calculated data, both the line half-widths and the temperature dependence coefficients, are available at the website ftp://ftp.iao.ru/pub/VTT/H2O-BT2-HW/BT2-296-Venus/.

The calculated data can be used in spectroscopy of the atmospheres of the Earth, Venus, and Mars. In the future, we intend to considerably improve the identification of calculation lists and the transition frequencies in much the same way as it was done in [31] for $HD^{16}O$.

ACKNOWLEDGMENTS

This work was supported in part by the Program 22.2 "Fundamental Problems of Research and Exploration of the Solar System" of the Presidium of the Russian Academy of Sciences and the Program 3.9 "Fundamental Optical Spectroscopy and Its Applications" of the Russian Academy of Sciences.

REFERENCES

1. J. B. Pollack, J. B. Dalton, D. Grinspoon, R. B. Wattson, R. Freedman, D. Crisp, D. A. Allen, B. Bezard, C. DeBergh, L. P. Giver, Q. Ma, and R. Tipping, Icarus **103**, 1 (1993).
2. M. D. Smith, J. Geophysical Research: Planets **107**, 5115 (2002).
3. T. Encrenaz, R. Melchiorri, T. Fouchet, P. Drossart, E. Lellouch, B. Gondet, J. -P. Bibring, Y. Langevin, D. Titov, N. Ignatiev, F. Forget, Astronomy and Astrophysics **441**, L9 (2005).
4. A. Fedorova, O. Korablev, J.-L. Bertaux, A. Rodin, A. Kiselev, S. Perrier, J. Geophysical Research: Planets **111**, E09S08 (2006).
5. A. A. Fedorova, S. Trokhimovsky, O. Korablev, and F. Montmessin, Icarus **208**, 156 (2010).
6. R. R. Gamache, S. P. Neshyba, J. J. Plateaux, A. Barbe, L. Regalia, J. B. Pollack, J. Mol. Spectrosc. **170**, 131 (1995).
7. L. R. Brown, C. M. Humphrey, and R. R. Gamache, J. Mol. Spectrosc. **246**, 1 (2007).
8. T. Fouchet, E. Lellouch, N. I. Ignatiev, F. Forget, D. V. Titov, M. Tschimmel, F. Montmessin, V. Formisano, M. Giuranna, A. Maturilli, and T. Encrenaz, Icarus **190**, 32 (2007).
9. B. Bezard, A. Fedorova, J.-L. Bertaux, A. Rodin, and O. Korablev, Icarus **216**, 173 (2011).
10. S. Chamberlain, J. Bailey, D. Crisp, and V. Meadows, Icarus **222**, 364 (2013).
11. C. Delaye, J.-M. Hartmann, and J. Taine, Appl. Opt. **28**, 5080 (1989).
12. B. Bezard, C. C. C. Tsang, R. W. Carlson, G. Piccioni, E. Marcq, and P. Drossart, J. Geophysical Research **114** E00B39 (2009).
13. J.-L. Bertaux, A.-C. Vandaele, O. Korablev, E. Villard, A. Fedorova, D. Fussen, E. Quemerais, D. Belyaev, A. Mahieux, F. Montmessin, C. Muller, E. Neefs, D. Nevejans, V. Wilquet, J. P. Dubois, A. Hauchecorne, A. Stepanov, I. Vinogradov, and A. Rodin, Nature **450**, 646 (2007).
14. A. Fedorova, O. Korablev, A. C. Vandaele, J. L. Bertaux, D. Belyaev, A. Mahieux, E. Neefs, W. V. Wilquet, R. Drummond, F. Montmessin, E. Villard, J. Geophysical Research: Planets **113**, E00B22 (2008).
15. V. A. Krasnopolsky, D. A. Belyaev, I. E. Gordon, G. Li, and L. S. Rothman, Icarus **224**, 57 (2013).
16. R. E. Novak, M. J. Mumma, and G. L. Villanueva, Planet. Space Sci. **59**, 163 (2011).
17. O. Korablev, A. V. Grigoriev, A. Trokhimovsky, Y. S. Ivanov, B. Moshkin, A. Shakun, I. Dziuban, Y. K. Kalinnikov, and F. Montmessin, Proc. SPIE—Int. Soc. Opt. Eng., 886709 (2013).
18. R. Drummond, A. C. Vandaele, F. Daerden, D. Fussen, A. Mahieux, L. Neary, E. Neefs, S. Robert, Y. Willame, and V. Wilquet, Planet. Space Sci. **59**, 292 (2011).
19. R. J. Barber, J. Tennyson, G. J. Harris, and R. N. Tolchenov, Mon. Not. R. Astron. Soc. **368**, 1087 (2006).
20. J. Bailey, Icarus **201**, 444 (2009).
21. J. Tennyson, M. A. Kostin, P. Barletta, G. J. Harris, O. L. Polyansky, J. Ramanlal, and N. F. Zobov, Comput. Phys. Commun. **163**, 85 (2004).

22. H. Sagawa, J. Mendrok, T. Seta, H. Hoshina, Ph. Baron, K. Suzuki, I. Hosako, C. Otani, P. Hartogh, and Y. Kasai, J. Quant. Spectrosc. Radiat. Transfer **110**, 2027 (2009).
23. L. R. Brown, C. M. Humphrey, and R. R. Gamache, J. Molec. Spectrocs. **246**, 1 (2007).
24. M. D. Smith, J. Geophys. Res. **107**, 25 (2002).
25. A. A. Fedorova, A. V. Rodin, and I. V. Baklanova, Icarus **171**, 54 (2004).
26. B. Bezard, A. Fedorova, J.-L. Bertaux, A. Rodin, and O. Korablev, Icarus **216** (1), 173 (2011).
27. L. S. Rothman, I. E. Gordon, Y. Babikov, A. Barbe, D. C. Benner et al., J. Quant. Spectrosc. Radiat. Transfer **130**, 4 (2013).
28. B. A. Voronin, N. N. Lavrentieva, T. P. Mishina, T. Yu. Chesnokova, M. J. Barber, and J. Tennyson, J. Quant. Spectrosc. Radiat. Transfer **111**, 2308 (2010).
29. B. A. Voronin, N. N. Lavrent'eva, A. A. Lugovskoi', A. D. Bykov, V. I. Starikov, J. Tennyson, Atmos. Oceanic Opt. **24** (11), 929 (2011).
30. A. S. Dudaryonok, B. A. Voronin, N. N. Lavrentieva, A. A. Lugovskoy, and V. I. Starikov, Proc. SPIE—Int. Soc. Opt. Eng. **8696**, 869604 (2012).
31. N. N. Lavrentyeva, B. A. Voronin, O. V. Naumenko, and A. A. Fedorova, Icarus **236**, 38 (2014).

Translated by V. Bulychev

SPELL: OK